

Scaling relations in early-type galaxies belonging to groups

Habib G. Khosroshahi^{1*}, Somak Raychaudhury¹, Trevor J. Ponman¹, Trevor A. Miles¹
& Duncan A. Forbes²

¹*School of Physics and Astronomy, The University of Birmingham, Birmingham B15 2TT, UK*

²*Centre for Astrophysics and Supercomputing, Swinburne University, Hawthorn, VIC 3122, Australia*

MNRAS submitted - September 2003

ABSTRACT

We present a photometric analysis of a large sample of early-type galaxies in 16 nearby groups, imaged with the Wide-Field Camera on the Isaac Newton Telescope. Using a two-dimensional surface brightness decomposition routine, we fit Sersic ($r^{1/n}$) and exponential models to their bulge and disk components respectively. Dividing the galaxies into three subsamples according to the X-ray luminosities of their parent groups, we compare their photometric properties. Galaxies in X-ray luminous groups tend to be larger and more luminous than those in groups with undetected or low X-ray luminosities, but no significant differences in n are seen. Both normal and dwarf elliptical galaxies in the central regions of groups are found to have cuspy profiles than their counterparts in group outskirts.

Structural differences between dwarf and normal elliptical galaxies are apparent in terms of an offset between their “Photometric Planes” in the space of n , r_e and μ_0 . Dwarf ellipticals are found to populate a surface, with remarkably low scatter, in this space with significant curvature, somewhat similar to the surfaces of constant entropy proposed by Márquez et al. (2001). Normal ellipticals are offset from this distribution in a direction of higher specific entropy. This may indicate that the two populations are distinguished by the action of galaxy merging on larger galaxies.

Key words: galaxies: fundamental parameters — galaxies: evolution — galaxies: dwarf — galaxies: elliptical and lenticular, CD — galaxies: structure — galaxies: groups — X-ray: galaxies: clusters

1 INTRODUCTION

Galaxy scaling relations, such as the Fundamental Plane, and its various projections, and the colour-magnitude relation have been used to enhance our understanding of galaxy structure and evolution. Early-type galaxies, in particular, form a relatively homogeneous population and hence rather well-defined scaling relations. Most large samples of early-type galaxies come from the rich environments of galaxies clusters. Studies of these high density regions benefit from the large numbers of galaxies in a small angular region of the sky (hence making observations more efficient) and from the morphology-density relation, which tells us that such environments are dominated by early-type galaxies. Thus our current knowledge gained from galaxy scaling relations applies mostly to clusters. The field and group environments are less well studied in this respect, and provide a means to study environmentally-dependent processes. For example, galaxy mergers (which can be about hundred times more efficient in today’s groups than clusters, cf. Mamon 1986) may result in merger-remnant Ellipticals that deviate strongly from the scaling relations

(e.g. Forbes, Ponman, & Brown 1998). On the other hand many of the well studied Elliptical galaxies are brightest group galaxies.

Recent X-ray observations of groups and their constituent galaxies have provided a new insight into the study of the evolution of galaxies in small ensembles and in intermediate-density environments (Helsdon & Ponman 2000; Mulchaey 2000). Miles et al. (2003) find that the shape of the luminosity function of galaxies in groups with low X-ray luminosity is significantly bimodal, in comparison with that of X-ray bright groups or rich clusters, showing a strong environmental effect on the morphological mix in a system, and on the evolution of galaxies in general. It is likely that the dip in the luminosity function at intermediate magnitudes arises from increased merging in low velocity dispersion systems.

Of particular interest in this context are early-type galaxies, which are more abundant in clusters and groups than in the field. Several well-known scaling relations (such as the Faber-Jackson relation or the Fundamental Plane of Elliptical galaxies) utilise galaxy velocity dispersions and hence require spectroscopic data. However, scaling relations like the Kormendy relation (Kormendy 1977) and the Photometric Plane of galaxies (Khosroshahi et al. 2000a) can be constructed from photometric observations alone.

There have been many studies aimed at understand-

* E-mail: habib@star.sr.bham.ac.uk

ing the differences in the structure of Ellipticals (E) and dwarf Ellipticals (dE), with mixed results. While some (e.g. Terlevich, Caldwell, & Bower 2001) argue in favour of the similarities between the two populations, others (e.g. Kormendy 1985) find evidence otherwise (see Graham & Guzmán 2003 for more details).

Traditionally, the surface brightness distribution of Ellipticals and bulges of disk galaxies have been modelled by the de Vaucouleurs profile. However, during the last decade, better photometry and advanced analysis have shown that their surface brightness distribution is, in general, better represented by the Sersic profile ($r^{1/n}$, Sersic 1968), of which the de Vaucouleurs profile ($r^{1/4}$) is a special case (Caon et al. 1993; Khosroshahi et al. 2000a; Graham 2001). The Sersic model is also widely used to describe the brightness distribution of bulges of disk galaxies (de Jong 1996; Andredakis et al. 1995; Khosroshahi et al. 2000b). The disk component of galaxies is usually characterised by an exponential distribution.

In this paper we examine the surface brightness distribution of Ellipticals belonging to galaxy groups, where most galaxies in the Universe reside. The relatively small number of galaxies in individual groups, compared to clusters, requires any analysis to be carried out on a large sample. This can be done in several ways. Here, the galaxies are classified based on the X-ray luminosity (L_X) of their parent groups, which, being correlated with the velocity dispersion of the group (e.g. Helsdon & Ponman 2000), can be an index of the dynamical state and the mass of the group (Miles et al. 2003; Osmond & Ponman 2003). The principal properties of the groups, and a detailed description of the sample can be found in section 2. The analysis techniques and morphology of galaxies is discussed in section 3. Correlations among various parameters and the scaling relations is studied in section 4. Section 5 contains a discussion and a summary of results.

2 OBSERVATIONS AND ANALYSIS

2.1 Observations

Our sample is drawn from the Group Evolution Multi-wavelength Study (GEMS, Osmond & Ponman 2003) of sixty groups, compiled by cross-correlating a list of over 4000 known groups from various studies with the list of archival ROSAT PSPC X-ray observations with integration > 10 ks. This includes several Hickson groups, as well as loose groups from the CfA survey. A large fraction of these were detected in the X-ray, and for the others we have upper limits for their X-ray luminosity.

Of the GEMS sample, 16 groups were observed at the 2.5m Isaac Newton telescope at the Roque de Los Muchachos Observatory, La Palma, between 2000 February 4–10. This is a random and representative subsample of the original sample of 60 groups, where all groups accessible for the allocated observing run were observed. The detector used was the Wide Field Camera (WFC), which is an array of four thinned EEV CCDs situated at the $f/3.29$ prime focus of the INT, each with an area of 2048×4096 pixels, each pixel being 0.33 arcsec across. Each CCD thus can image an area of 22.5×11.3 arcmin of sky, together covering 1017 sq.arcmin.

Photometry was performed with broadband BRI filters, of which we analyse only the R -band images here. Our analysis is limited to galaxies brighter than $M_R = -13$. The median seeing achieved was about 1.1 arcsec in R . Further details can be found in (Miles et al. 2003).

Table 1. The sample of 16 groups used in this study

Group	R.A. (J2000)	Dec. (J2000)	N ^a	Distance ^b Mpc	log L_X ^c ergs/s
HCG 10	01:25:40.4	+34:42:48	45	68.2	41.75
HCG 68	13:53:26.7	+40:16:59	177	41.1	41.67
NGC 524	01:24:47.8	+09:32:19	27	35.4	41.09
NGC 1052	02:41:04.8	-08:15:21	10	20.3	41.03
NGC 1587	04:30:39.9	+00:39:43	54	55.2	41.22
NGC 2563	08:20:35.7	+21:04:04	149	73.5	42.54
NGC 3227	10:23:30.6	+19:51:54	18	26.5	40.88
NGC 3607	11:16:54.7	+18:03:06	26	23.5	41.09
NGC 3640	11:21:06.9	+03:14:06	56	28.5	<40.34
NGC 3665	11:24:43.4	+38:45:44	41	37.2	41.15
NGC 4151	12:10:32.6	+39:24:21	14	23.0	<40.15
NGC 4261	12:19:23.2	+05:49:31	43	34.8	41.84
NGC 4636	12:42:50.4	+02:41:24	24	13.1	41.73
NGC 4725	12:50:26.6	+25:30:06	7	25.1	41.00
NGC 5044	13:15:24.0	-16:23:06	55	34.4	43.08
NGC 5322	13:49:15.5	+60:11:28	18	32.4	41.51

^aNumber of member galaxies within our imaging field identified by the colour selection outlined in § 2.2.

^bDistance measured from the mean redshift of group (assuming $H_0 = 70$ km s⁻¹Mpc⁻¹; $q_0 = 0.5$), corrected for local bulk flows.

^cBolometric X-ray luminosity from Osmond & Ponman (2003)

2.2 Group Membership

The identification of the group galaxies is based on a colour selection. Source extraction was performed using the SExtractor software Bertin & Arnouts (1996), which uses a routine based on neural network generated weights for star-galaxy separation. Detections were checked visually and objects with the *stellaricity* parameter greater than 0.9 were deemed to be definitely stellar and therefore discarded. To obtain colours, a fixed aperture, set to be slightly greater than the seeing, was used to evaluate fluxes with different filters. All objects with FWHM less than the mean seeing were not processed further.

Galaxies were selected as being likely group members on the basis of their $B - R$ colour. A conservative cut of $B - R = 1.7$ was found to remove the majority of background galaxies for all groups in our sample (See Miles et al. 2003 for further details). Those galaxies found in the NASA/IPAC Extragalactic Database (NED) within the virial radius R_{vir} (see Osmond & Ponman 2003).

2.3 Analysis

The core of our data analysis is the two-dimensional decomposition of galaxies, by fitting a Sersic profile to the bulge and an exponential profile to the disk component, for obtaining the structural photometric parameters, and morphological classification. This analysis was carried out on all galaxies identified as group members using the selection method described in the previous section.

The bulge-disk decomposition procedure used here involves fitting two-dimensional image models to the observed galaxy images, assumed to consist of a bulge and a disk component. The model image is convolved with a Gaussian PSF, with the FWHM measured from the galaxy frame. Details of the accuracy and reliability of the decomposition procedure, and the associated galaxy simulation code, can be found in Wadadekar et al. (1999).

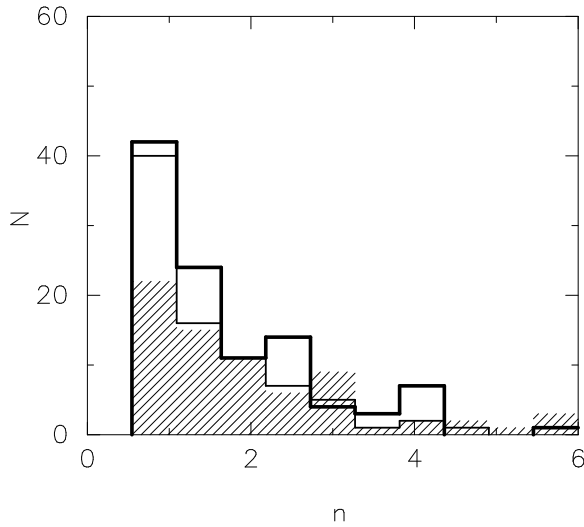


Figure 1. Distribution of the Sersic parameter n for early-type galaxies ($B/T > 0.5$) in our sample, in X-ray bright (bold line), X-ray dim (thin line) and X-ray undetected groups (those with no discernible group emission, shaded histogram). There is no significant difference in the n distribution between the types of groups.

The Sersic profile for the bulge is given by

$$I_{\text{bulge}}(x, y) = I_b(0) \exp[-2.303 b_n (r_{\text{bulge}}/r_e)^{1/n}]; \quad (1)$$

$$r_{\text{bulge}} = \sqrt{x^2 + y^2 / (1 - \epsilon_b)^2}.$$

Here x and y are the distances from the centre of the galaxy along the major and minor axis respectively. The quantity b_n is a function of n , and is evaluated as a root of an equation involving the incomplete gamma function (Wadadekar et al. 1999). It is well approximated by

$$b_n = 0.87 n - 0.14. \quad (2)$$

For $n = 4$, which corresponds to the de Vaucouleurs law, $b_4 = 3.33$. We model the disk intensity by the Freeman (1970) exponential distribution,

$$I_{\text{disk}}(x, y) = I_d(0) \exp(-r_{\text{disk}}/r_d); \quad (3)$$

$$r_{\text{disk}} = \sqrt{x^2 + y^2 / (1 - \epsilon_d)^2}.$$

The disk is assumed to be intrinsically circular, with the observed ellipticity ϵ_d of the disk in the observed image being due to projection effects alone.

The free parameters of the fit are:

- (i) The central bulge intensity $I_b(0)$,
- (ii) The half-light radius of the bulge r_e ,
- (iii) The ellipticity of the bulge ϵ_b ,
- (iv) The bulge shape parameter n (Sersic profile),
- (v) The central intensity of the disk $I_d(0)$,
- (vi) The scale length of the disk r_d , and
- (vii) The ellipticity of the disk ϵ_d .

Additional parameters such as sky background and position angle are estimated in a preliminary fit and are then held fixed during the final fitting process.

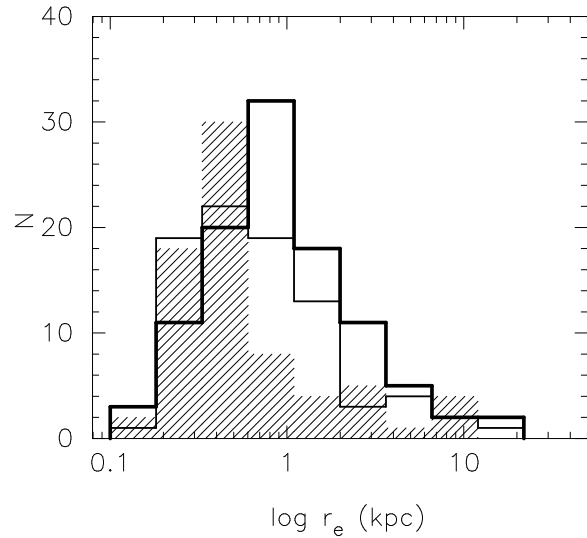


Figure 2. Distribution of the half-light radius r_e for early-type galaxies, in X-ray bright (bold line), X-ray dim (thin line) and X-ray undetected groups (shaded histogram). This shows that X-ray bright groups contain a larger proportion of galaxies that are bigger than their counterparts in X-ray dim or undetected groups.

3 MODELLING THE TWO-DIMENSIONAL SURFACE BRIGHTNESS OF GALAXIES

We were able to obtain satisfactory fits with a reduced $\chi^2_{\nu} \leq 2$ for 471 galaxies from our initial sample of 764 galaxies. Any fit with a reduced $\chi^2_{\nu} > 2$ is considered to be unacceptable and the galaxy excluded from the sample. Such unacceptable fits result mainly from irregularities in the brightness distribution, or from the presence of multiple nuclei or close companions. Such features cannot be represented by the simple and smooth models used in this study.

3.1 Morphological classification

The galaxies with satisfactory fits to the surface brightness model are assigned morphological types based on their bulge-to-total luminosity ratio, B/T . An ideal Elliptical galaxy has $B/T = 1$ and a late-type disk galaxy has a value of B/T close to zero.

We classify a galaxy as early-type when it has $B/T > 0.5$. This criterion was chosen to be $B/T > 0.4$ by Balogh et al. (2002), but the conclusions of this study are not sensitive to such a difference in selection. An ‘‘Elliptical galaxy’’ is one with $B/T \geq 0.95$. A galaxy with $B/T < 0.1$ is considered as a pure disk galaxy with an exponential luminosity profile, since the bulge in this case is too small to be modelled by the Sersic profile.

3.2 Galaxies in X-ray bright, dim and undetected groups

The X-ray luminosities of the parent groups in our sample are taken from Osmond & Ponman (2003), who measured them by fitting two-dimensional β -profiles to ROSAT PSPC observations in the 0.5–2 keV range, extrapolated to estimate the bolometric X-ray luminosity. Point sources were removed from the data before luminosity calculations and the values have then been corrected for flux lost in this process using the surface brightness models.

Since the number of galaxies in each group is small, we obtain statistical results by grouping galaxies according to X-ray brightness of their parent groups. We have divided the groups to be X-ray

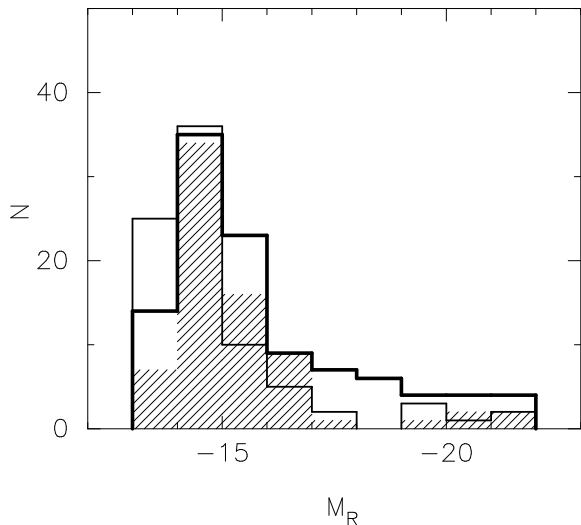


Figure 3. Distribution of the absolute R magnitude for early-type galaxies ($B/T > 0.5$) in our sample. The three categories are the same as in Figs. 1 & 2. This shows that X-ray bright groups contain a higher fraction of brighter galaxies than X-ray dim or undetected groups.

bright or dim according to their bolometric X-ray luminosity being more or less than the median of the sample, $L_X = 10^{41.7}$ erg/s. This luminosity refers to the X-ray luminosity of the group plus any central galaxy that might exist. In addition, we have a third category of group (called X-ray undetected) where there is no discernible “group emission”, and all the diffuse emission, if any, can be accounted for as due to individual non-central galaxies in the group.

There are 189, 174 and 108 galaxies (out of 316, 298 and 150) with acceptable profile fits in the categories of X-ray bright, dim and undetected groups respectively. Since the sample covers a wide range of X-ray luminosity, here we seek possible differences in the properties of galaxies that depend on their local environment characterised by L_X .

3.3 Variation in brightness profiles with galaxy environment

Figure 1 shows the distribution of the Sersic parameter for early type galaxies ($B/T > 0.5$) in X-ray bright, dim and undetected groups. There is no significant difference in the distribution of values of the Sersic parameter n among X-ray bright, dim and undetected groups, corroborated by the K-S statistics.

The difference, in the distribution of the half-light radius r_e of bulges of early-type disk galaxies, between the various categories of parent groups, is substantial. Figs. 2 and 3 show the distribution of r_e and M_R in the three sub-samples in this study, indicating that X-ray bright groups contain a larger fraction of galaxies that are bigger and more luminous than their counterparts in X-ray dim groups. This is confirmed by the K-S test performed on the distributions of r_e and M_R . The underdensity of early-types implied by the gap in the histograms for X-ray dim and undetected groups in Fig. 3 around $M_R = -18$ is due to the dip in the LF of these groups, discussed in further detail by Miles et al. (2003).

The Sersic parameter n is often found to be correlated with the absolute magnitude of the Elliptical galaxies (Young & Currie 1994; Binggeli & Jerjen 1998), which would indicate that the Sersic parameter is an intrinsic property of a galaxy. Here, we find a highly scattered correlation between n and M_R for Elliptical galax-

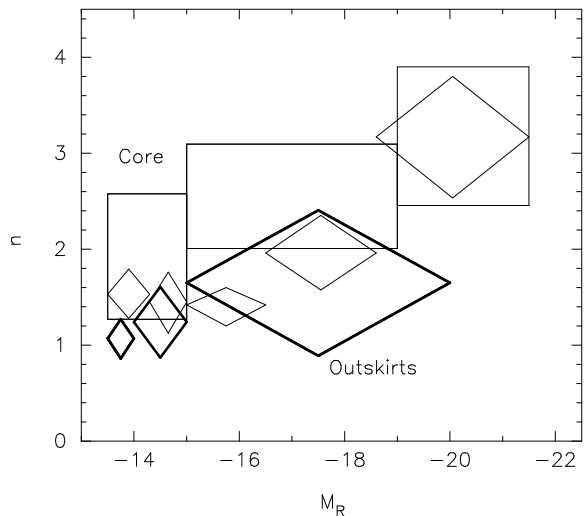


Figure 4. The correlation between the Sersic parameter n and the absolute R magnitude of the Elliptical galaxies in our sample. The width of the diamonds represent bins chosen to include 10 galaxies in each. The height of each diamond represents the 95% confidence level around the mean values of the Sersic parameter n in the bin. The dotted and bold diamonds represent galaxies at the core ($R/R_{\text{vir}} < 0.15$) and in the outskirts ($R/R_{\text{vir}} > 0.6$) of the groups, and thin diamonds represent galaxies in between.

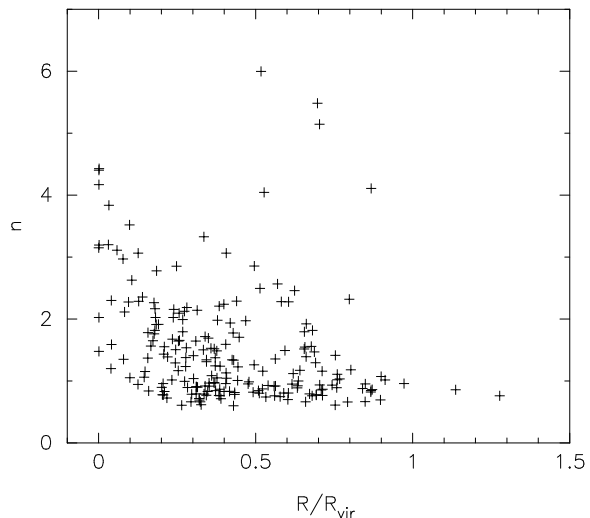


Figure 5. The Sersic parameter n of each Elliptical galaxy, plotted against the normalised projected distance from the centre of its parent group. This behaviour is expected if the value of n is correlated with the local three-dimensional galaxy density.

ies (both E and dE) in groups, with a scatter of about 1.5 mag in M_R , which is much larger than the scatter (about 0.45 mag in M_B) found by Young & Currie (1994).

In order to understand the origin of this scatter in the $n - M_R$ relation, we plot the galaxies as a function of their normalised projected distance from the centre of their parent group (Fig. 4). Since the distribution of the Sersic parameter does not show a significant variation with X-ray properties of the group, we use galaxies belonging to all three sub-samples together to improve statistics. Galaxies in the core of the groups ($R/R_{\text{vir}} < 0.15$) have higher values for the Sersic parameter (mean value and 95% confidence level of $1.92^{+0.66}_{-0.65}$), while in the outer regions ($R/R_{\text{vir}} > 0.6$), galax-

ies have lower values of n and hence are less cuspy (mean value and 95% confidence level of $1.07^{+0.20}_{-0.21}$). The systematic variation in values of n with the distance from the centre of the parent group appears to be independent of how bright the galaxies are.

Trujillo et al. (2002) recently found a triangular distribution between the concentration index of galaxies (related to n) and the projected two-dimensional local density of galaxies in clusters, which is expected even if n (and concentration parameter) and M_R were tightly correlated. At higher projected densities, galaxies with both low and high values of concentration index will be binned together due to projection. On the other hand, since galaxies in low-density environments have low n , at lower projected densities only galaxies with lower values of concentration index will be seen.

Fig. 5 shows a similar triangular distribution between the Sersic parameter n and normalised projected distance for the galaxies in our sample. If n and M_R of Elliptical galaxies were correlated for normal and dwarf Ellipticals, Fig. 5 would seem to indicate that the dwarf Ellipticals are preferentially removed from the core of each group, but enhanced in the outer regions. However, from Fig 4 it appears that the situation is more complicated. We find faint dEs ($M_R > -15.0$), with relatively higher values of n , at smaller normalised projected distances from the centre of the groups. This might suggest that these high- n dEs are at the core of their groups. This strongly suggests that environmental effects can play a key role in the shape of the light profile (characterised by values of n), in galaxies and that this parameter is not an intrinsic property of a galaxy.

This also shows that dEs, traditionally known to have near-exponential brightness profiles, can have cuspy cores, and can exist in the central regions of groups. These “nucleated” dEs have been found to be more centrally concentrated in their distribution in detailed studies of nearby clusters, e.g. Virgo and Fornax (Ferguson & Binggeli 1994). It is interesting to note that such cusps are also known to exist in starburst dEs (e.g. Summers, Stevens, & Strickland 2001).

4 PHOTOMETRIC SCALING RELATIONS

One of the essential observational ingredients of the study of galaxy evolution is the family of scaling relations such as the Fundamental Plane, characteristic of dynamically relaxed Elliptical galaxies (Djorgovski & Davis 1987; Dressler et al. 1987). Although the Fundamental Plane for bright Elliptical galaxies is found to be scarcely affected by environmental factors, it may not be so for low mass Ellipticals. While Nieto et al. (1990) showed that dwarf Ellipticals¹ follow the same trend defined by the Fundamental Plane of bright Elliptical galaxies, albeit with a larger scatter due to structural variation, the dwarf Ellipticals in Virgo cluster studied by Peterson & Caldwell (1993) belong to a different Fundamental Plane.

In the absence of spectroscopic measures of velocity dispersion, which is a key parameter in constructing the Fundamental Plane, one can study those projections of the Fundamental Plane which are purely photometric. In this section, we will study the photometric characteristics of the Elliptical galaxies in our sample (those with $B/T \geq 0.95$, as defined in §3.1), a subset of our sample of “early-type galaxies” ($B/T \geq 0.5$)

¹ Unless otherwise stated, in this paper we will refer to Ellipticals fainter than $M_R = -18$ as dwarfs (dEs) and those brighter as normal Ellipticals (Es).

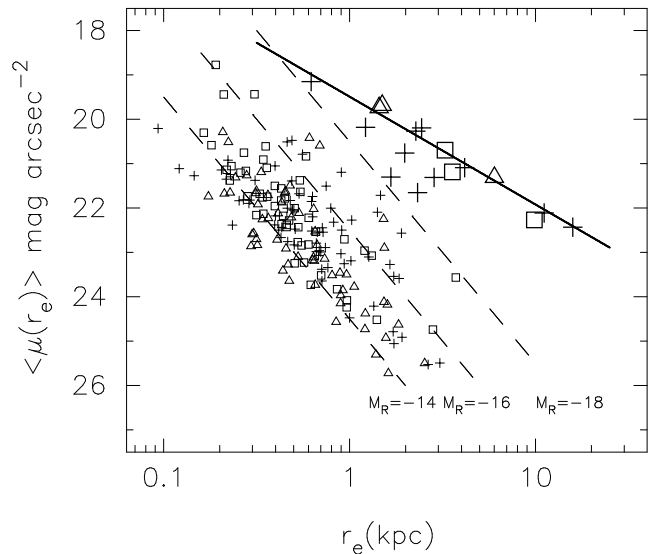


Figure 6. The Kormendy relation for Elliptical galaxies in X-ray bright (crosses), X-ray dim (triangles) and X-ray undetected groups (squares). Large symbols are for galaxies with $M_R < -18$. The solid line represents the KR for bright Ellipticals in the Coma cluster with central velocity dispersion $\sigma > 200$ km/s (Ziegler et al. 1999). Dashed lines represent lines of constant absolute magnitude, our limit being $M_R = -13$.

4.1 The Kormendy relation

Elliptical galaxies are known to show a strong correlation between the mean surface brightness $\langle \mu_e \rangle$, and the half-light radius r_e , known as the Kormendy relation (KR) $\langle \mu_e \rangle = A_K \log r_e + B_K$, with the slope A_K lying in the range 2.0–3.0 (Kormendy 1977). The Kormendy relation for cluster Ellipticals shows a r.m.s. scatter of about 0.1 dex, which would result in a 25% error in r_e and hence in measuring distance to the galaxies.

Fig. 6 shows the Kormendy relation for Elliptical galaxies in our sample, where galaxies belonging to parent groups which are X-ray bright ($L_X > 10^{41.7}$ erg/s), X-ray dim and X-ray undetected are plotted with different symbols. The plot shows two distinct populations: the “normal” Ellipticals ($M_R < -18$, mean KR slope $\sim 2.3 \pm 0.4$) and the dwarf Ellipticals ($-18 < M_R < -13$, mean KR slope $\sim 4.1 \pm 0.2$). However, from Fig. 6, it is apparent that instead of a linear KR, we may interpret the distribution of dEs as one of high scatter, truncated by our magnitude limit ($M_R \leq -13$).

We also note that there are very few galaxies in the zone between the two populations, which results from the significant dip in the luminosity function of groups in the range $-16 > M_R > -18$, as seen in Miles et al. (2003).

Comparing with the KR for galaxies in rich clusters, we find that the slope of the KR for our brightest galaxies ($M_R < -19.5$) 2.75 ± 0.16 , compared to 2.43 ± 0.15 for a similar sample in the Coma cluster (Ziegler et al. 1999, plotted as the solid line in Fig. 6).

Extending the KR plot of the Coma cluster to fainter galaxies (e.g. Graham & Guzmán 2003), Ellipticals in the magnitude range $-15 > M_B > -18$ are found to follow a trend, at almost constant r_e , quite distinct from that of the brighter galaxies, the latter having a slope similar to that found in our sample. Our sample of dwarfs extends to fainter $M_R \approx -13$ smaller ($r_e \approx 100$ pc) galaxies, and shows the presence of substantial scatter in both axes. Some contribution to this large scatter may also arise from dependencies on local environment, since we are merging galaxies from 16 groups in a single plot. Our conclusion (in agreement with

Graham & Guzmán (2003)) is that the Kormendy relation in itself does *not* provide strong evidence for any fundamental difference in structure between normal and dwarf Ellipticals.

4.2 The Photometric Plane

Recent developments in the study of the structure of galaxies and the modelling of brightness profiles, in particular with the use of the more general Sersic model, provides a unified description of the photometric properties of normal (E) and dwarf Ellipticals (dE), traditionally seen as two distinct families (e.g. Kormendy 1985). The discontinuity between these two extreme exponential ($n \sim 1$, dEs) and de Vaucouleurs profiles ($n \sim 4$, Es) is now filled by both populations possessing a large range of values $1 < n < 6$. The bulges of disk galaxies share the same Photometric Plane with Ellipticals.

The Photometric Plane (PP, Khosroshahi et al. 2000a) is a bivariate relation that links only photometric parameters, obtained by fitting a Sersic model to a galaxy image, $\log n = A \log r_e + B \mu_0$. Our simulations show that fitting galaxy brightness distributions with unsuitable models (e.g. the de Vaucouleurs model to a galaxy where $n \neq 4$), can result in a significant variation in the values of structural parameters. For example, assuming $n = 4$ in the case of a $n = 2$ galaxy can result in a change in the value of half-light radius by a factor of three. Thus it is important to allow for a free parameter n to account for the cusp and core in Ellipticals or bulges of disk galaxies.

Most scaling relations, e.g. the Kormendy relation or the Fundamental Plane, are insensitive to these variations, since the three parameters of the Sersic model (μ_0 , n , r_e) are correlated and their combinations used in these scaling relations are robust (Bertin et al. 2002). The Photometric Plane, on the other hand, allows us to explore the entire range of these parameters for Elliptical galaxies, and thus can be used more effectively as a tool to examine the connection between structural parameters and the evolutionary history of galaxies.

The Photometric Plane for all Ellipticals in our sample is given by

$$\log n = (0.21 \pm 0.09) \log r_e - (0.074 \pm 0.013) \mu_0 + (1.7 \pm 0.3). \quad (4)$$

This equation is similar to that found for the bright Elliptical galaxies in the K -band study of 42 Coma galaxies (Khosroshahi et al. 2000a). However, the scatter in n here is 0.13 *dex*, much larger than the scatter found for the Coma cluster sample, which is 0.05 *dex*, which can be attributed to the fact that our sample is dominated by dEs. To verify this, we examine the Ellipticals with $M_R < -18$ in X-ray bright groups (comparable to the Coma sample), to find that the scatter about the Photometric Plane for Es is only 0.06 *dex* in $\log n$, compared to 0.10 *dex* for dEs. The fact that the scatter around the the Photometric Plane of normal Es is lower than that of dEs indicates that Es and dEs are structurally different systems even though their n values might be similar.

We plot the principal axes (K_1 , K_2 , K_3) of the Photometric Plane against each other in Fig. 7, where $K_1 = 0.99 \log n + 0.17 \log r_e$, $K_2 = 0.16 \log n - 0.92 \log r_e - 0.38 \mu_0$ and $K_3 = -0.06 \log n + 0.37 \log r_e - 0.93 \mu_0$ (directly comparable to the similar plot for Coma Ellipticals in Khosroshahi et al. 2000a). Since this sample has a fainter magnitude limit, it probes the PP for dwarfs more extensively, and demonstrates that the PP for the dEs has a strikingly low scatter (in contrast, for example, to their scat-

ter in the Kormendy plot). This strongly suggests that dEs might be a more homogeneous class than is normally thought, and follow well-defined structural trends.

To explore a more direct connection with the underlying physical changes in galaxy structure between Es and dEs, we turn to a slightly different version of these correlations in the next section.

4.3 The Specific Entropy Plane

Márquez et al. (2001), in their study of cluster Ellipticals, showed that the Photometric Plane is close to a plane of constant specific entropy of galaxies, originally introduced by Lima Neto et al. (1999). Although self-gravitating systems like galaxies do not possess stable states of absolute maximum entropy, the evolution of entropy via two-body relaxation will be a slow process, and Márquez et al. (2000) argue that the violent relaxation process which occurs during galaxy formation may establish a quasi-equilibrium state of constant specific entropy, and they find evidence that both simulated and observed galaxies do indeed show approximately constant entropy per unit mass. In the case of observed galaxies, the properties of the Photometric Plane result from this approximate constancy of specific entropy.

On examination of the surfaces of constant entropy in detail, it is found that they actually exhibit some curvature when represented in the coordinate system of the PP. It can be seen, from the two edge-on views of our plane in Fig. 7, that there are clear indications of curvature in the distribution of the dwarfs. This curvature, rather than stochastic scatter, accounts for much of the larger variance about the plane for dEs (compared to normal Es) discussed in section 4.2. Could this curvature be indicating that dwarfs really follow a surface of constant specific entropy? In Fig. 8 we plot a representation of the Photometric Plane in terms of $1/n$, for our sample, using Eq. (4) above, and overlay a line of constant specific entropy. The latter has been calculated using Eqs. (23) & (24) of Márquez et al. (2001), in conjunction with the relevant relations from their Appendix A. Here, we have only adjusted the value of the specific entropy parameter (s_0) to find the curve which best matches our data.

The curvature seen in the distribution of dwarfs in Fig. 8 is similar to that the constant s_0 surface, although the shape does not match in detail. It is also apparent that the normal Es fall above the dwarfs in the Figure, which corresponds to the direction of increasing s_0 . The dashed line corresponds to a specific entropy Plane with $s_0 = -25$ for our sample of Elliptical galaxies dominated by dEs.

5 DISCUSSION AND CONCLUSIONS

This study confirms earlier results that massive Ellipticals show higher values of the Sersic parameter n , *i.e.* a cuspiers surface brightness profile at their centre (Young & Currie 1994). From the large scatter in the plot of absolute R magnitude and n (Fig. 4), we conclude that the shape of the radial profile, represented by the value of n , is not uniquely related to the intrinsic luminosity of the galaxy. Furthermore, the dependence of n on the location of galaxies within their groups (Fig. 4) shows that environmental dependence is responsible for part of this scatter. Although we find no significant difference between the values of n in groups of different X-ray luminosity, we do find that for both dEs and Es (though not the most luminous Es), surface brightness profiles tend to be cuspiers (higher n) for galaxies located in the cores of groups. One

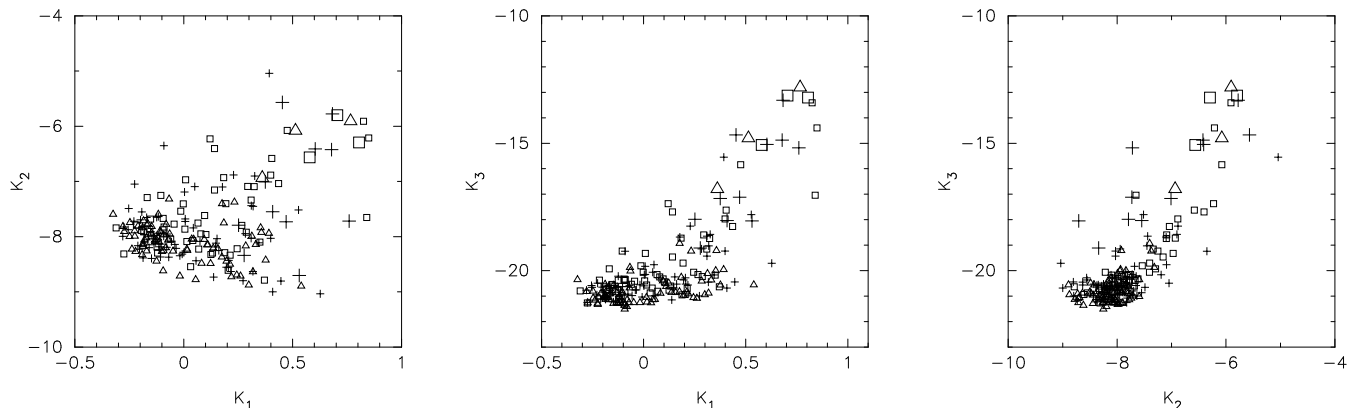


Figure 7. The face-on and two edge-on views of the Photometric Plane for Ellipticals in our sample. The symbols have the same meaning as in Fig.6. the principal axes K_1 , K_2 and K_3 are defined in §4.2.

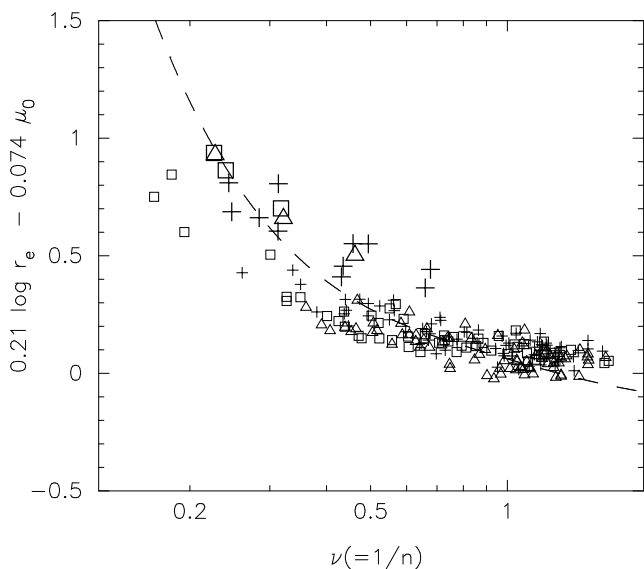


Figure 8. The Photometric and Specific Entropy Planes of Elliptical galaxies in X-ray bright (crosses), X-ray dim (triangles) and X-ray undetected groups (squares). Large symbols are for galaxies with $M_R < -18$. The dashed curve is the best match Specific Entropy Plane with $s_0 = -25$.

explanation for this correlation could be the effects of interaction-induced star formation in triggering nuclear starbursts within more centrally located galaxies.

Normal Ellipticals in groups are found to yield similar Photometric Plane and Kormendy relation parameters to those in rich clusters. There is no difference in the Kormendy relation or Photometric Plane between Ellipticals belonging to the different classes of X-ray bright, faint or undetected groups. Furthermore, the Kormendy relation is found to be of little value in distinguishing structural differences between dEs and Es, since the KR slope found for dwarfs is dominated by selection effects, most notably the magnitude limit of the sample. The sparse region in the KR plot, separating dEs and Es, is easily interpreted as resulting from the dip seen in the galaxy luminosity function at $M_R \sim -18$, and discussed in more detail in Miles et al. (2003).

Dwarf and normal Ellipticals are distinguished much more effectively in terms of their location in the Photometric Plane in the space of n , r_e and μ_0 . The dwarfs inhabit a non-flat surface in

this space, with a curvature somewhat akin to a surface of constant specific entropy, as defined by the equations of Márquez et al. (2001), though the match is only approximate. Even if galaxies do have constant specific entropy, a degree of mismatch between observation and the analytical expressions of Márquez et al. (2001) is not surprising, given the numerous assumptions (e.g. mass-traces-light, and isotropic velocities) which have been made in deriving the equations of the isentropic surfaces. The well-defined nature of the locus followed by these dwarfs is a strong indicator of their structural coherence, and the larger scatter that they exhibit about their Photometric Plane is largely due to the curvature of the surface they inhabit, rather than to a large random scatter in their properties. Normal galaxies, on the other hand, are offset relative to the dwarf locus, in a direction corresponding to higher specific entropy. In this context, it is interesting that Márquez et al. (2000) find, from their simulations, that merging tends to increase specific entropy. Hence the offset may indicate that normal Ellipticals, which fall above the dip seen in the galaxy luminosity function, have undergone mergers, whilst dwarfs have not. This supports the idea (Miles et al. 2003) that merging may have played a role in generating the dip in the luminosity function, by converting middle-ranking galaxies into larger ones, whilst dwarfs are largely unaffected due to their smaller merger cross-sections.

ACKNOWLEDGMENTS

We would like to thank Ale Terlevich for help in observation and basic data reduction, John Osmond for making the results of his analysis available for us and Yogesh Wadadekar for the use of his 2D decomposition code.

REFERENCES

- Andredakis, Y.C., Peletier, R.F., & Balcells, M. 1995, MNRAS, 275, 874
- Balogh M.L., Smail I., Bower R.G., Ziegler B.L., Smith G.P., Davies R.L., Gaztelu A., Kneib J.-P. and Ebeling H., 2002, ApJ, 566, 123
- Bertin G. & Arnouts, S., 1996, A&AS, 117, 393
- Bertin G., Ciotti L. and Del Principe M. 2002, A&A, 386, 149
- Binggeli B. and Jerjen H., 1998, A&A, 333, 17
- Burstein, D. 1979, ApJS, 41, 435

- Caon, N., Capaccioli, M. & D'Onofrio, M. 1993, MNRAS, 163,1013
- de Jong, R. S. 1996, A&AS, 118, 557
- dell'Antonio I.P. Geller M.J. and Fabricant D.G., 1994, AJ, 107, 427
- de Vaucouleurs, G. 1948, Ann. d'Astrophys., 11, 247
- Djorgovski, S.G. & Davis, M. 1987, ApJ, 313, 59
- Dressler A. et al.1987, ApJ, 313, 42
- Faber, S. M., and Jackson, R. E. 1976, ApJ, 204, 668
- Ferguson, H. C. & Binggeli, B. 1994, A&A Rev., 6, 67
- Forbes, D. A., Ponman, T. J., & Brown, R. J. N. 1998, ApJ, 508, L43
- Freeman, K. 1970, ApJ, 160, 811
- Graham A. W. & Guzmán R., 2003, AJ, 125, 2936
- Graham A. W., 2001, AJ, 121, 820
- Graham A. W., Trujillo I. and Caon N., 2001, AJ, 122, 1707
- Guzmán R., Graham A.W., Matkovic A., Vass I., Gorgas J. and Cradial N, 2003, astro-ph/0303390
- Helsdon S. F. & Ponman T. J. 2000, MNRAS, 315, 356
- Jorgensen I., Franx M. and Kjaergaard P., 1995, MNRAS, 276, 1341
- Jorgensen I., Franx M. and Kjaergaard P., 1996, MNRAS, 280, 167
- Khosroshahi H. G., Wadadekar Y., Kembhavi A. and Mobasher B. 2000a, ApJ, 531, L103
- Khosroshahi H. G., Wadadekar Y. and Kembhavi A. 2000b, ApJ, 533, 162
- Kormendy, J. 1977, ApJ, 217, 406
- Kormendy, J. 1985, ApJ, 295, 73
- Lima Neto G. B., Gerbal D. and Marquez I. 1999, MNRAS, 309, 481
- Mamon, G. A. 1986, ApJ, 307, 426
- Márquez I., Lima Neto G. B., Capelato H., Durret F., Gerbal D., 2000, A&A, 353, 873
- Márquez I., Lima Neto G. B., Capelato H., Durret F., Lanzoni B., Gerbal D., 2001, A&A, 379, 767
- Miles T. A., Raychaudhury S., Forbes, D., Goudfrooij, P., Ponman, T.J., 2003, submitted to MNRAS
- Mulchaey J. S. 2000, ARAA, 38, 289
- Nieto J.-L., Bender R., Davoust E. and Prugniel P. 1990, A&A, 230, L17
- Osmond, J.P.F. & Ponman T.J., 2003, submitted to MNRAS
- Peterson R.C. and Caldwell N., 1993, AJ, 105, 1411
- Sersic, J.L. 1968, Atlas de galaxias australes. Observatorio Astronómica, Cordoba
- Summers, L. K., Stevens, I. R., & Strickland, D. K. 2001, MNRAS, 327, 385
- Terlevich, A. I., Caldwell, N., & Bower, R. G. 2001, MNRAS, 326, 1547
- Trujillo I., Aguerri J.A.L., Gutierrez C.M. and Cepa J., 2001, AJ, 122, 38
- Trujillo I., Aguerri J.A.L., Gutierrez C.M., Caon N. and Cepa J., 2002, ApJ, 573L, 9
- Wadadekar Y., Robbason R., & Kembhavi A. 1999, AJ, 117, 1219
- Young C.K. and Currie M.J. 1994, MNRAS, 268, L11
- Ziegler B.L., Saglia R.P., Bender R., Belloni P., Greggio L. and Seitz S., 1999, A&A, 346, 13